TCP1 promotes the progression of malignant tumors by stabilizing c-Myc through the AKT/GSK-3β and ERK signaling pathways

Yuanzhong Chen (chenyz@fjmu.edu.cn)
Fujian Medical University Union Hospital https://orcid.org/0000-0003-1298-6391

Hekun Liu
Fujian Key Laboratory of Translational Research in Cancer and Neurodegenerative Diseases, Institute for Translational Medicine, The School of Basic Medical Sciences, Fujian Medical University

Linying Chen
Department of Pathology, the First Affiliated Hospital of Fujian Medical University

Yiyi Jin
Fujian Key Laboratory of Translational Research in Cancer and Neurodegenerative Diseases, Institute for Translational Medicine, The School of Basic Medical Sciences, Fujian Medical University

Xiance Chen
Fujian Key Laboratory of Translational Research in Cancer and Neurodegenerative Diseases, Institute for Translational Medicine, The School of Basic Medical Sciences, Fujian Medical University

Nengjun Ma
Fujian Key Laboratory of Translational Research in Cancer and Neurodegenerative Diseases, Institute for Translational Medicine, The School of Basic Medical Sciences, Fujian Medical University

Fan Yang
Fujian Key Laboratory of Translational Research in Cancer and Neurodegenerative Diseases, Institute for Translational Medicine, The School of Basic Medical Sciences, Fujian Medical University

Huixia Bi
Fujian Key Laboratory of Translational Research in Cancer and Neurodegenerative Diseases, Institute for Translational Medicine, The School of Basic Medical Sciences, Fujian Medical University

Wenwen Liu
Fujian Key Laboratory of Translational Research in Cancer and Neurodegenerative Diseases, Institute for Translational Medicine, The School of Basic Medical Sciences, Fujian Medical University

Xinxin Wen
Fujian Key Laboratory of Translational Research in Cancer and Neurodegenerative Diseases, Institute for Translational Medicine, The School of Basic Medical Sciences, Fujian Medical University

Xinyan Li
Fujian Key Laboratory of Translational Research in Cancer and Neurodegenerative Diseases, Institute for Translational Medicine, The School of Basic Medical Sciences, Fujian Medical University

Shenmin Xu
Fujian Key Laboratory of Translational Research in Cancer and Neurodegenerative Diseases, Institute for Translational Medicine, The School of Basic Medical Sciences, Fujian Medical University
Hongliang Xu
Fujian Key Laboratory of Translational Research in Cancer and Neurodegenerative Diseases, Institute for Translational Medicine, The School of Basic Medical Sciences, Fujian Medical University
Juan Chen
Fujian Key Laboratory of Translational Research in Cancer and Neurodegenerative Diseases, Institute for Translational Medicine, The School of Basic Medical Sciences, Fujian Medical University
Yanping Lin
Fujian Key Laboratory of Translational Research in Cancer and Neurodegenerative Diseases, Institute for Translational Medicine, The School of Basic Medical Sciences, Fujian Medical University
Yuwen Chen
Fujian Key Laboratory of Translational Research in Cancer and Neurodegenerative Diseases, Institute for Translational Medicine, The School of Basic Medical Sciences, Fujian Medical University
Yinghong Yang
Department of Pathology, Fujian Medical University Union Hospital
Yong Wu
Fujian Institute of Hematology, Fujian Provincial Key Laboratory on Hematology, Fujian Medical University Union Hospital

---

Article

Keywords: Molecular chaperone TCP1, c-Myc, AKT/GSK-3β, ERK, ubiquitination

Posted Date: August 1st, 2022

DOI: https://doi.org/10.21203/rs.3.rs-1742161/v1

Abstract

TCP1, one of the subunits of molecular chaperone containing tailless complex polypeptide 1 (CCT) (CCT1), maybe play an essential role in cell proliferation and tumorigenesis. However, the biological functions and the underlying mechanisms of TCP1 in tumors are not fully understood. Here, we found that TCP1 levels increased with successive generations of xenografted tumors and were associated with the tumorigenicity of HL-60 cells. TCP1 expression was significantly higher in *de novo* and recurrent leukemia clinical samples and in various solid tumor tissues than in their related normal tissues. High expression of TCP1 was significantly associated with poor outcomes in patients with pancreatic ductal adenocarcinoma (PDAC) and HCC. Functional assays and mechanistic studies revealed that TCP1 suppression not only decreased the proliferation and invasion of cancer cells *in vitro* but also inhibited tumor growth and metastatic spread *in vivo.* Ubiquitination assays and mechanistic studies revealed that TCP1 regulated the stability of c-Myc through the AKT/GSK-3β and ERK signaling pathways. Moreover, TCP1 knockin (TCP1-KI) mice, which generated by CRISPR/Cas9-mediated genome engineering, dramatically facilitated the occurrence of DEN-induced HCC. Our results demonstrate a novel mechanism of TCP1 regulation in multiple malignant tumors, and targeting TCP1 may provide new therapeutic strategies for the cancer treatment.

Introduction

Molecular chaperone containing tailless complex polypeptide 1 (CCT) is the main component in maintaining a proteostasis network. It plays an important role in protein biosynthesis, folding, translocation, assembly, degradation, and protein homeostasis through a complex cooperative mechanism[1,2]. CCT contains eight subunits (CCT1-CCT8), forming a chaperone ring structure [3,4]. Previous studies have shown that the high expression of CCT subunits is closely related to the occurrence and development of cancers[5–11]. Importantly, increasing evidence indicates that CCT mediates the development and progression of cancer by interacting with oncogenic factors that regulate tissue growth and apoptosis[12–16], indicating that CCT may participate in the process of cancer as a regulatory factor of proto-oncogenes. Our studies have indicated that TCP1, one of the subunits of CCT (CCT1), may be a potential biomarker for hepatocellular carcinoma (HCC), we demonstrated that TCP1 regulates Wnt7b/β-catenin pathway through P53 to influence the proliferation and migration of hepatocellular carcinoma cells [17]. However, little is known about the function of TCP1 in the pathogenesis of cancers other than HCC, such as leukemia and pancreatic ductal adenocarcinoma (PDAC).

As mentioned previously, TCP1 could not only assist in the folding of proteins as a chaperone but can also regulate the anti-oncogene p53. Thus, we speculate that TCP1 may also regulate other cancer-related genes (including oncogenes and anti-oncogenes) in the progression of tumors. The stabilization and degradation of oncogenic proteins are essential for tumor formation, development, and metastasis[18]. As a multifunctional transcription factor, the c-Myc oncoprotein is hyperactivated in most human cancers and is closely associated with a poor clinical prognosis in patients [19,20]. The stabilization of c-Myc is

related to tumor initiation and tumor progression in various cancers, including PDAC and HCC[19, 21]. The stability and activity of the c-Myc protein are strictly regulated by phosphorylation-dependent degradation in the ubiquitin-proteasome system. The phosphorylation of threonine 58 (Thr58) and serine 62 (Ser62) of the c-Myc protein is involved in regulating its stability[22]. A variety of signaling pathways have been identified to modulate the phosphorylation of c-Myc, thereby affecting its protein stability and function in cells. For example, the PI3K/AKT pathway, which is commonly mutated in cancers [23], could modulate c-Myc protein stability via a series of transduction cascades[24–27]. GSK-3β, a downstream effector of the PI3K/AKT pathway, is inhibited by AKT-mediated phosphorylation at residue Ser9[26]; AKT can phosphorylate c-Myc at residue Thr58 and then ubiquitinate the c-Myc protein. In addition, the Ser62 residue of c-Myc can be phosphorylated by extracellular regulated protein kinases (ERKs) or cyclin-dependent kinases (CDKs), stabilizing the c-Myc protein in cells [28,29]. The stabilization of c-Myc increases its transcriptional activity, promoting the expression of downstream target genes[30]. However, whether and how TCP1 regulates the stability of c-Myc to participate in the progression of cancers remains unknown.

In the present study, we identified that TCP1 may be a crucial marker in the carcinogenesis process which increased the tumorigenic rate from 30–100% in generation by generation tumorigenesis model, we demonstrated that increased expression of the TCP1 protein was significantly associated with tumorigenesis in human leukemic cell lines *in vivo*. We showed that TCP1 was prevalently overexpressed in multiple human solid cancers and that high TCP1 expression indicated shorter survival in PDAC patients. Genetic TCP1 inhibition significantly decreased the proliferation, migration, and invasion of PDAC and HCC cells *in vitro* and *in vivo* by regulating the stability of c-Myc via the AKT/GSK-3β and ERK signaling pathways, respectively. Furthermore, TCP1 potently promoted primary HCC induced by diethylnitrosamine (DEN) in TCP1 knockin (TCP1-KI) mice. Taken together, our studies demonstrated the role of TCP1 in both human leukemia and several solid cancers. It might function as a tumor-promoting factor, play a crucial role in the process of tumorigenesis, and offer a promising therapeutic target for cancers.

Materials And Methods

Cell lines and animals

The human malignant hematological cell lines HL-60, Kasumi, KG1-α, NB4, CA46, HEL, and U266; the human pancreatic carcinoma cell lines PANC-1 and BxPC-3; and the hepatoma cell lines SMMC-7721 and Huh-7 were purchased from the National Collection of Authenticated Cell Cultures (Shanghai, China). HL-60, Kasumi, KG1-α, NB4, CA46, HEL, U266, BxPC-3, and SMMC-7721 cells were cultured in RPMI 1640 medium. PANC-1 and Huh-7 cells were maintained in DMEM. All cells were cultured in complete medium supplemented with 10% fetal bovine serum (FBS, HyClone, Logan, Utah, USA) and 1% penicillin/streptomycin (HyClone, Logan, Utah, USA) at 37°C in a 5% CO_2 humidified incubator.

Six- to eight-week-old BALB/c nu/nu mice purchased from Shanghai Laboratory Animal Co., Ltd. (SLAC, Shanghai, China) were raised in specific pathogen-free conditions. BALB/c nude mice were housed in laminar flow cabinets with free access to food and water in the Laboratory Animal Center of Fujian Medical University (FJMU). All animal experiments were performed following the animal protocols and regulations approved by the Animal Ethics Committee of FJMU.

Patients and specimens

Bone marrow samples were collected from healthy donors and acute myeloid leukemia (AML) patients from the Hematology Department of the FJMU Union Hospital. AML was diagnosed according to the French-American-British (FAB) classification[31]. All of the patients and healthy donors signed informed consent forms. In addition, all samples of solid tumors, including gastric cancers, liver cancers, pancreatic cancers, lung cancers, lymphoma, and thyroid carcinoma were collected from the FJMU Union Hospital or First Affiliated Hospital of FJMU between 2015 and 2017. No patient received chemotherapy or radiotherapy before the operation. Overall survival (OS) was defined as the duration from the date of initial diagnosis to the date of death. None of the patients died within 1 month after surgery. Tissue slides were cut into 4-μm sections for immunochemistry (IHC) and immunofluorescence (IF), and all sections were examined and scored independently by two investigators in a double-blinded manner. Staining intensity was determined according to a histological scoring method. We quantified the staining intensity and the percentage of stained cells, and positive tumor cells were quantified by two independent pathologists. Staining intensity was scored from 0 to 3: negative (0), weak (1), medium (2), and strong (3). The degree of staining (the percentage of positive staining area of tumor cells in the whole tumor area) was scored as 0 (0%), 1 (1–25%), 2 (26–50%), 3 (51–75%) or 4 (76–100%). The total protein expression score (overall score range, 0–12) was calculated by multiplying the intensity and degree of staining scores.

Generation by generation tumorigenesis model and construction of highly tumorigenic HL-60 cells

Xenotransplantation was performed in nude mice to develop a generation by generation tumorigenesis model and generate highly tumorigenic HL-60 cells. Briefly, HL-60 cells (2×10^6 cells/100 μl PBS) were implanted subcutaneously into ten nude mice to form tumors. The mice were observed for one month and then sacrificed under aseptic conditions; the tumor tissues were cut into approximately 0.5×0.5-cm pieces. The tissues were digested for approximately 5 min, and then tumor cells (designated as HL-60-G1) were cultured *in vitro*. After 15 passages of subculture, the cells were implanted into the outer part of the right hind limb of nude mice again, and then the solid tumors were removed aseptically and cultured to generate stable HL-60-G2 cells. The procedure was repeated twice to obtain four generations of cell lines (until the tumor formation rate increased to 100%), and then tumor cells obtained from the mice (designated as HL-60-G4) were cultured *in vitro*.

Proteomic analysis

Two-dimensional differential in-gel electrophoresis (2D-DIGE) and protein identification were performed as previously described[32]. Five cell samples derived from HL-60, HL-60-G0, HL-60-G1, HL-60-G2, HL-60-G3, and HL-60-G4 cells were used for proteomic analysis. The HL-60 cell sample was set as a control. Four highly tumorigenic HL-60 cell samples were randomly labeled with Cy3 or Cy5, whereas internal standards were labeled with Cy2 using 400 pmol of fluorochrome/50 μg of protein. Cy3- and Cy5-labeled samples were combined before mixing with Cy2-labeled internal standard and separated by 2D-DIGE. After 2D-DIGE, the gels were scanned on a Typhoon 9410 scanner. Normalization and quantification of protein spots in the gels were carried out with Decyder 6.5 software. The resulting peptides were identified with a 4800 Proteomics Analyzer for matrix-assisted laser desorption/ionization-time of flight (MALDI-TOF) mass spectrometry and tandem TOF/TOF mass spectrometry. The above cell protein extraction, separation, and identification protocols were performed in the Beijing Proteome Research Center (Beijing, China).

Western blotting (WB) and Real-time quantitative PCR (RT-qPCR)

WB was performed using the standard method, as reported previously[33]. Anti-GAPDH antibody was used as a loading control to normalize the levels of other proteins. All antibodies are listed in Supplemental Table S1.

Total RNA in cells was extracted using TRIzol reagent (Invitrogen, Carlsbad, CA, USA) and reverse transcribed into complementary DNA with the PrimeScript Reverse Transcriptase kit (Takara, Dalian, China). RT-qPCR was performed on a 7500 Real-Time PCR system with a SYBR Real-Time PCR kit (Takara). All primers are listed in Supplemental Table S2. The relative gene expression level was calculated using the $2^{-\Delta\Delta CT}$ method.

Construction of lentivirus containing the shTCP1 vector

The optimal sequences of TCP1 short hairpin RNA (shRNA) were as follows:

TCP1-shRNA/F: 5’ CCGG GGTGTACAGGTGGTCATTATTCAAGAGATAATGAC CACCTGTACACCTTTTTTG 3’

TCP1-shRNA/R: 5’ AATT CAAAAAAGGTGTACAGGTGGTCATTATCTCTTGAA TAATGACCACCTGTACACC 3’. A negative control with no homology to the human genome was created as a scrambled sequence. The packaging plasmids pVSVG, pREV, and pMDL; shTCP1; and the control plasmid PLKO.1-puro were transfected into HEK293T cells. Freshly plated cells were infected with the lentivirus, and the knockdown efficiency for the target genes was determined by WB or RT-qPCR.

Cell proliferation

Cell proliferation was determined by 3-(4,5-dimethylthiazol-2-yl)-2,5-diphenyltetrazolium bromide (MTT) assay and cell colony formation assay. The MTT assay was performed using standard techniques, as reported [34]. For the cell colony formation assay, the number of colonies containing 50 or more cells was

counted under a light microscope. The colony formation rate was calculated as the proportion of colonies/seeded cells.

Transwell assays

For the Transwell assays, 2×10^5 cells were suspended in 200 μL of serum-free medium and then seeded into the upper chamber without or with Matrigel for migration or invasion assay. The lower chamber was filled with 800 μL of whole medium. Following incubation for 36 h, the cells that had migrated or invaded through the membrane were fixed and stained with 0.1% crystal violet and counted under a microscope.

Ubiquitination assay

Cells (transfected with scrambled shRNA and shTCP1) were transiently transfected with Flag-c-Myc and HA-ubiquitin using TurboFect transfection reagent (Thermo Fisher Scientific) according to the manufacturer's instructions for 35 h. All cells were treated with MG-132 for 1 hour; subsequently, cells were lysed with IP lysis buffer and boiled at 95°C for 10 min. The supernatant was transferred to a new tube and incubated with Flag-tagged antibody and protein A/G agarose to purify the transfected c-Myc protein. The precipitate was analyzed by WB with anti-HA to detect the ubiquitinylated c-Myc protein.

Subcutaneous xenograft tumor model in nude mice

The subcutaneously transplanted nude mouse model was constructed as previously described[33]. Briefly, cells (2×10^6) were subcutaneously injected into the bilateral upper flank regions of the nude mice. Tumor volume was calculated every 3 days following the formula: volume = $1/2\times\text{length}\times\text{width}^2$. When the tumor volume reached 1000 mm^3, the mice were sacrificed, and the tumors were removed to calculate the size and weight.

In vivo metastatic assays in nude mice and bioluminescence imaging (BLI)

SMMC-7721 and BxPC-3 cells were transfected with lentivirus labeled with the luciferase and shTCP1. SMMC-7721 and BxPC-3 cells stably expressing luciferase (2×10^6 cells) were suspended in 100 μl PBS and injected into nude mice via the tail vein. The lung metastasis was monitored by BLI using an IVIS Spectrum In Vivo Imaging System (PerkinElmer, Santa Clara, CA, USA) starting 2 weeks after implantation.Fifteen minutes before BLI, animals were injected intraperitoneally with D-luciferin (150 mg/kg). The experiments were performed every two weeks for 8 weeks.

Transgenic mice and primary hepatocarcinoma model

The mouse TCP1 gene is located on mouse chromosome 17, and the mouse ROSA26 gene is located on mouse chromosome 6. The "CAG-mouse TCP1 CDS-poly A" targeting vector was inserted into the ROSA26 gene intron 1 to produce TCP1-KI mice. To engineer the targeting vector, homology arms will be generated by PCR using BAC clone from the C57BL/6 library as template. Cas9 and gRNA will be co-injected into

fertilized eggs with targeting vector. Cas9 specifically cut the ROSA26 gene intron sequence under the guidance of gRNA, then the "CAG-mouse TCP1 CDS-poly A" targeting vector was inserted into the ROSA26 gene intron by homologous recombination for KI mice production. The pups will be genotyped by PCR followed by sequencing analysis. Wild-type (WT) and TCP1-KI mice (C57BL/6J background) were purchased from Cyagen Biosciences Inc. (Suzhou, China). For the DEN-induced HCC model, 15-day-old male mice were intraperitoneally injected with DEN (dissolved in PBS, 25 mg/kg body weight). After 12 months, the mice were euthanized, and liver tissues were dissected and used for follow-up experiments. The number of tumor nodules, the ratio of liver weight, and the tumor volume were evaluated in a blinded manner between WT and TCP1-KI mice that were not randomly allocated. Then, HE, IHC, and WB assays were used to detect the related indexes using standard techniques.

Statistical analysis

Statistical analyses were performed using SPSS 22.0 and GraphPad Prism 5 software packages. Quantitative data between groups were compared using Student's t-test (two-sided) or one-way ANOVA. The differences in gene expression levels between AML patients and normal controls and the correlations between gene expression and clinical features were analyzed by the Mann-Whitney U test or chi-square test. Survival data in mice were presented using Kaplan-Meier curves, and significance was estimated using the log-rank test (GraphPad Prism). The data shown in the bar chart are the mean and standard deviation (SD). Differences with $P < 0.05$ were considered statistically significant.

Results

The level of TCP1 increases with successive generations of xenograft tumors and is associated with the tumorigenicity of HL-60 cells in vivo

Previous studies have indicated that successive implantation of HL-60 cells in nude mice could increase tumor formation *in vivo*. However, the underlying mechanisms are still unclear. For this purpose, we established four generations of HL-60 cell lines according to previous descriptions [35]. As expected, the four generations of HL-60 cell lines exhibited increasing subcutaneous tumor formation ability with tumor formation rates of 30% (3/10) for HL-60-G1, 50% (5/10) for HL-60-G2, 80% (8/10) for HL-60-G3 and 100% (10/10) for HL-60-G4 cells (Fig. 1A). To address the possible molecular changes during the acquisition of tumorigenicity, five cell lysates were prepared and subjected to 2D-DIGE combined with mass spectrometry for proteomic analysis (Fig. 1B). The results of 2D-DIGE showed up to 2153 matched protein spots on the gels. Among these, 33 spots were significantly upregulated in the highly tumorigenic cells, whereas 54 spots were downregulated (Supplementary Fig. 1A). One differentially expressed protein, master No. 71, was identified as TCP1 via MALDI-TOF/TOF MS analysis (Supplementary Fig. 1B). To further verify TCP1 expression in tumor nodules, we performed IHC staining to detect TCP1 protein in tumor tissues formed by different generations of tumor cells. As shown by IHC analysis, the expression of TCP1 increased with increasing generations (Fig. 1C), which suggested that TCP1 may be closely related to the formation of malignant tumors. We then tested this hypothesis in tissue samples with AML and a

variety of leukemia cells. RT-qPCR and WB showed that the expression of TCP1 in the initial untreated and recurrent marrow samples of AML was significantly higher than that in AML bone marrow samples in the normal and remission stages (Fig. 1D, E). The expression level of TCP1 in various malignant hematological cells was also higher than that in normal bone marrow specimens (Fig. 1F). The results indicate that TCP1 is highly expressed in leukemia cells and is related to the tumorigenicity of HL-60 cells *in vivo*.

TCP1 is highly expressed in many solid tumors and is related to poor outcomes in patients with PDAC and HCC

Given the upregulated expression of TCP1 in AML patients and leukemic cell lines (Fig. 1) and HCC[17], we speculated that TCP1 might be upregulated in various malignant solid tumors. To explore the clinical significance of TCP1, we examined the expression of TCP1 in PDAC, HCC, lung cancer, lymphoma, gastric cancer, and thyroid cancer. The average level of TCP1 in tumor tissues was higher than that in adjacent tissues in all types of cancer examined (Fig. 2A), indicating that TCP1 is markedly increased in many solid tumors. Subsequently, we focused on the expression of TCP1 in pancreatic cancer and liver cancer by IHC and immunofluorescence (IF). The results showed that the expression of TCP1 in poorly differentiated PDAC and HCC[17] was higher than that in well-differentiated and moderately differentiated tumors (Fig. 2B, C, F), and the overall survival (OS) time of patients with high levels of TCP1 was significantly shorter than that of patients with low levels of TCP1 (Fig. 2D). Pearson correlation analysis showed that the TCP1 level was negatively correlated with recurrence time in patients with PDAC and HCC (Fig. 2E, G), suggesting that TCP1 is associated with poor prognosis of malignant tumors.

Suppression of TCP1 inhibits the proliferation, migration, and invasion in PDAC and HCC cells

To investigate the effect of TCP1 on the phenotype of PDAC and HCC cells, we conducted functional experiments to evaluate the influence of TCP1 knockdown on cell proliferation, migration, and invasion. First, BxPC-3, PANC-1, SMMC-7721, and Huh-7 cells were infected with lentivirus containing shRNA targeting TCP1. TCP1 protein expression was significantly decreased in all shTCP1 cell lines (Fig. 3A). MTT and colony formation assay results showed that shTCP1 significantly inhibited cell growth and colony formation (Fig. 3B, C). Next, we examined the effect of shTCP1 on cell migration by Transwell assays. shTCP1 significantly inhibited the migration and invasion in four cells types (Fig. 3D). Thus, TCP1 knockdown successfully attenuated the proliferation, migration, and invasion of various cancer cell models *in vitro*.

Suppression of TCP1 expression inhibits tumor growth and metastatic spread in animal models

To explore the effect of altered TCP1 expression on the processes of tumor proliferation, we established a xenograft model in nude mice using PANC-1, SMMC-7721, and Huh-7 cancer cell lines. Consistent with the *in vitro* results, xenograft tumors with downregulated TCP1 expression grew more slowly than the control xenografts (Fig. 4A). Compared with the controls, TCP1 suppression showed significant growth inhibition as tumor volume decreased and tumor weight was lost in all three cell lines (Fig. 4B, C). To

further investigate the role of TCP1 in PDAC and HCC metastasis, we injected SMMC-7721 and BxPC-3 cells labeled with luciferase into the mice by tail veins to track their metastasis. The metastatic ability of pancreatic cancer and liver cancer cells *in vivo* was detected by a living imaging system. As illustrated, knocking down TCP1 significantly reduced metastatic spread in both SMMC-7721 and BxPC-3 cells (Fig. 4D, E). Furthermore, the OS rates of mice treated with shTCP1 cancer cells were significantly longer than those of the control mice (Fig. 4F). In conclusion, these results suggest that knockdown of TCP1 could significantly decrease tumor burden *in vivo*.

TCP1 inhibition accelerates the degradation of c-Myc via the ubiquitin-proteasome pathway

Our *in vitro* and *in vivo* results showed that TCP1 had a strong effect on tumor cell proliferation. To better understand the molecular mechanism of TCP1-mediated tumor progression, we examined whether TCP1 inhibition affects the core signaling networks that are known to play an important role in HCC and PDAC, including PI3K/AKT/mTOR, MAPK signaling pathways and the key genes of cell proliferation. According to the results of the WB (Supplementary Fig. 2), we assessed the influence of TCP1 on the expression of the tumor proliferation-related protein c-Myc in TCP1 knockdown cell models. The results showed that the protein level of c-Myc but not the mRNA level was significantly decreased (Fig. 5A, B). Therefore, we speculated that TCP1 could affect the stability of the c-Myc protein. Subsequently, we used the protein synthesis inhibitor cycloheximide (CHX) to measure the degradation of the c-Myc protein. We found that the degradation of c-Myc was faster in cancer cells with TCP1 knockdown than in control cells, implying that TCP1 may regulate the protein stability of c-Myc (Fig. 5C). Then, MG132 was added to inhibit the activity of the 26S proteasome. The degradation of c-Myc protein was significantly inhibited in cancer cell models treated with both CHX and MG132 compared with those treated with CHX alone (Fig. 5C). Moreover, we observed that the degradation rate of c-Myc was considerably accelerated in the shTCP1 group compared with the scramble group in all types of cancer examined (Fig. 5D). Successively, using ubiquitination assays, we found that TCP1 knock-down increased the ubiquitination level of c-Myc (Fig. 5E). Thus, the above results indicated that suppression of TCP1 expression promotes the ubiquitination of c-Myc in cells, which eventually accelerates the degradation of the c-Myc protein.

TCP1 regulates the stability of c-Myc through AKT/GSK-3β and ERK signaling pathways

Previous studies have pointed out that the phosphorylation of Thr58 decreases the stability of c-Myc and promotes its degradation via the ubiquitin-proteasome pathway; the phosphorylation of Ser62, on the other hand, stabilizes c-Myc[28,29]. It has been reported that the phosphorylation of c-Myc is regulated mainly by the AKT/GSK-3β and ERK pathways[22]. To determine whether TCP1 regulates c-Myc protein stability through its phosphorylation, we manipulated TCP1 expression levels in above four cell lines and determined changes in the phosphorylation of c-Myc. While the total protein level of c-Myc and the ratio of p-c-Myc Ser62 to p-c-Myc Thr58 were decreased in TCP1 knockdown cells, TCP1 overexpression showed the opposite effect, providing evidence that TCP1 regulates the stability of c-Myc mainly by altering the ratio of p-c-Myc Ser62 to p-c-Myc Thr58 (Fig. 6A-D). Then, we assessed the levels of key proteins of the AKT/GSK-3β and ERK signaling pathways. The phosphorylation of AKT Ser473, GSK-3β Ser9, and ERK was significantly reduced with TCP1 knock-down but increased with TCP1 overexpression

(Fig. 6A, C). However, the total protein levels of AKT, GSK-3β, and ERK were not changed in either TCP1 knock-down or overexpression cells (Fig. 6A, C). These results suggest that TCP1 regulates the AKT/GSK-3β and ERK signaling pathways. After knocking down TCP1 and inhibiting GSK-3β activity with AR-A014418 (AR), the protein level of c-Myc was restored, which demonstrated that TCP1 regulates the stability of c-Myc by modulating the AKT/GSK-3β signaling axis (Fig. 6E, F). Next, we used different concentrations of the AKT-specific inhibitor AKT inhibitor VIII (AKT-iVIII) to inhibit AKT activity in the four cell lines, we found that the TCP1 protein levels were not changed (Fig. 6G), which indicates that the TCP1 protein is an upstream regulator of the AKT/GSK-3β pathway. These results revealed that TCP1 regulates the stability of the c-Myc protein through the AKT/GSK-3β and ERK signaling pathways, elucidating the mechanism of TCP1 in pancreatic cancer and liver cancer.

Overexpression of TCP1 promotes the expression of c-Myc by regulating the AKT/GSK-3β and ERK signaling pathways, thus promoting the occurrence of primary liver cancer

To gain global insight into the mechanism of TCP1 in hepatocarcinogenesis, WT and TCP1-KI mice were used to construct the primary HCC model induced by DEN. The number of tumor nodules (the red arrows), the ratio of liver weight, and tumor volume significantly increased in TCP1-KI group compared with WT group (Fig. 7A, B), indicating that TCP1 promotes the occurrence and development of primary HCC. Histological analysis showed that the liver tissues of the TCP1-KI group had no complete liver lobules (Fig. 7C). The nuclei of the hepatocytes were enlarged, and the vacuolation was seriously disordered compared with that in WT group (Fig. 7C). TCP1-KI group showed obvious pathological features of hepatoma. In addition, IHC showed that the expression of c-Myc and Ki67 was significantly increased in the TCP1-KI group (Fig. 7C). Furthermore, the influence of TCP1 overexpression on the AKT/GSK-3β and ERK pathways was noted by WB. The overexpression of TCP1 could activate the AKT/GSK-3β and ERK pathways to promote the expression of c-Myc (Fig. 7D), which further confirmed our hypothesis *in vivo*.

Here, we discovered an important role for TCP1 in promoting cancer cell proliferation and metastasis through c-Myc. TCP1 increased the phosphorylation of ERK, leading to the phosphorylation of c-Myc Ser62, which could promote cell proliferation. Moreover, the level of phosphorylated c-Myc Thr58 was significantly decreased after TCP1 upregulated the phosphorylation of AKT/GSK-3β, which led to the inhibition of c-Myc degradation (Fig. 8). Taken together, our findings reveal a novel mechanism of TCP1 and indicate that TCP1 may be a valuable molecular marker for cancer diagnosis and prognosis evaluation.

Discussion

In the present study, we showed that the tumorigenicity of HL-60 cells was increased with successive generations in animal models. Surprisingly, proteomic analysis indicated that the key underlying molecular change involved the TCP1 protein. In addition to the changes in TCP1 in animal models, our studies also found that TCP1 expression was upregulated not only in leukemia clinical samples but also

in various human malignant hematological cell lines, which suggests that TCP1 may be involved in the process of tumorigenesis and the development of tumors.

Recently, growing evidence has demonstrated that the molecular chaperone CCT is a critical mediator of tumorigenesis[14, 36–42]. Although the function of CCT has been widely studied, the effect of its subunit, especially TCP1, on cancer and its specific mechanism are still unclear. Thus, we focused on TCP1 to further explore how this subunit of CCT regulates tumor progression. In this study, we reported that TCP1 was markedly elevated in malignant tumors such as PDAC, HCC, lung cancer, lymphoma, gastric cancer and thyroid gland cancer. TCP1 was identified as a poor prognostic indicator for both time to recurrence and OS in PDAC and HCC in this and our previous studies[17], and the results further support the function of TCP1 in cancers as an oncogene.

Cancer is characterized by uncontrolled proliferation and metastasis[43,44]. Thus, inhibiting the proliferation and metastasis of tumor cells is a crucial therapeutic strategy. Here, functional experiments demonstrated that knockdown of TCP1 dramatically inhibited the growth and metastasis of tumors *in vitro* and *in vivo*. The results revealed the functions of TCP1 in tumor cells and highlighted its role in cancers. Given these findings, we considered that TCP1 might contribute to the tumorigenesis and progression of cancers as an oncogene.

Although TCP1 is associated with the progression of cancers, the mechanism by which TCP1 promotes the development of tumors has not been delineated. On the other hand, as an oncogenic transcription factor, c-Myc regulates various biological activities, including proliferation, apoptosis, and carcinogenesis[45–49]. Accumulating evidence has confirmed that c-Myc can be activated by many mechanisms in cancer cells, including transcription regulation, mRNA stabilization, and protein overexpression and stabilization[50]. Thus, treatments targeting c-Myc may hinder the rapid proliferation of cancer cells[51–53]. However, therapeutics directly targeting c-Myc are not yet available. We focused on the stability of c-Myc in our studies considering that the high rate of its degradation could acutely regulate the activity of c-Myc[54]. Our results showed that the protein level of c-Myc was notably reduced after TCP1 knockdown without affecting the mRNA level, illustrating the role of TCP1 in c-Myc protein stability.

In this context, our results further demonstrated that the degradation rate of c-Myc in pancreatic and liver cancer cells was dramatically increased after knocking down TCP1 and treating cells with CHX. In addition, the expression of the c-Myc protein could be rescued by MG132. These results further demonstrated that TCP1 could regulate the degradation of c-Myc protein via the proteasome pathway. Ubiquitination assays then revealed that knocking down TCP1 not only affects the degradation rate of c-Myc but also promotes the ubiquitination of c-Myc in cells. Considering the essential functions of c-Myc in tumorigenesis, it is not surprising that the degradation of c-Myc could ultimately result in the suppression of cancers. The results suggested that c-Myc is a link between TCP1 and tumorigenesis. TCP1 could modulate the progression of cancers by regulating the stability of c-Myc, which offers vital insights into the pathogenic mechanism of cancers.

The findings were further supported by analysis of the phosphorylation sites. The stability and activity of the c-Myc protein are strictly regulated by its two conserved phosphorylation sites, Thr58 and Ser62. ERK phosphorylates c-Myc at the Ser62 residue and increases its protein stability. GSK-3β phosphorylates c-Myc at the Thr58 residue and promotes its degradation[27,28]. In addition, GSK-3β is regulated by PI3K/AKT through Ser9 phosphorylation. The phosphorylation of GSK-3β inhibits its ability to phosphorylate c-Myc at Thr58, thereby stabilizing c-Myc[22,55,56]. AKT/GSK-3β and ERK pathways have a critical function in cancer proliferation, invasion, and drug sensitivity[57–59]. We showed that AKT/GSK-3β, p-AKT, p-GSK-3β, c-Myc and the ratio of p-c-Myc Ser62 to p-c-Myc Thr58 were downregulated when TCP1 was knocked down in liver and pancreatic cancer cells. The phosphorylation of ERK in the ERK pathway was also decreased. The results were reversed when TCP1 was overexpressed in cancer cells. These results revealed that TCP1 regulates the stability of the c-Myc protein through the AKT/GSK-3β and ERK signaling pathways and, for the first time, highlighted the effect of changes in the ratio of p-c-Myc Ser62 to p-c-Myc Thr58, which indicates a unique mechanism of TCP1.

More importantly, to further elucidate the mechanism of TCP1 in HCC, TCP1-KI genetically engineered mice were used to construct a primary HCC model induced by DEN. The results were consistent with those *in vitro*, which further confirmed the mechanism of TCP1 in cancers and provided a novel theoretical basis for research on TCP1 and the treatment of cancers. Collectively, our identification of TCP1 should be a starting point to explore its functions, adding a new dimension to our understanding of molecular chaperones and facilitating the development of novel therapeutic strategies for tumors.

In summary, our data demonstrated that the expression of TCP1 in liver cancer and pancreatic cancer was closely associated with a poor prognosis in patients. Knocking down TCP1 could regulate the phosphorylate c-Myc at Thr58 and Ser 62 and further inhibit the malignant phenotype of liver cancer and pancreatic cancer cells via AKT/GSK-3β and ERK signaling pathways. Genetically engineered mice were then utilized to verify the results. For the first time, we confirmed the effect of TCP1 on the AKT/GSK-3β and ERK axes. This study shows that TCP1 is linked to HCC and PDAC via the stabilization of c-Myc. Overall, this study not only describes a new TCP1 function in cancer-related genes but also provides a unique strategy for tumor treatment through the inactivation of TCP1 to facilitate c-Myc ubiquitination, which suggests that TCP1 acts not only as a member of the type II chaperone CCT but also as a tumor susceptibility factor in cancer development.

Declarations

ACKNOWLEDGEMENTS

This work was supported by the Joint Funds for the Innovation of Science and Technology, Fujian Province (2017Y9054), the Fujian Provincial Department of Science and Technology (2019J01442), and the Startup Fund for scientific research, Fujian Medical University (2020QH2007).

AUTHOR CONTRIBUTIONS

Y.C., H.L. and Y.W. conceived the study, generated hypotheses and designed experiments; H.L., L.C., Y.J., X.C., N.M., J.C. and Y.L. performed the cell experiments; Y.W., X.C., F.Y., X.L., S.X., H.B. and W.L. engaged in the animal experiments and H.L., Y.Y., X.W. and H.X. conducted he clinical experiments; L.C., Y.J. and X.W. participated in data analysis; H.L., L.C. and Y.J. drafted and embellished the manuscript.

CONFLICT OF INTEREST

The authors declare no competing interests.

ETHICAL APPROVAL AND CONSENT TO PARTICIPATE

This study was approved by the Biomedical research ethics review committee of FJMU (FJMU200918) and the Ethics Committee of Fujian Medical University Union Hospital(2017KY091), and informed consent was obtained from all participants.

References

1. Balch, W.E., Morimoto, R.I., Dillin, A. & Kelly, J.W. Adapting proteostasis for disease intervention. Science **319**, 916–919 (2008).
2. Morimoto, R.I. Proteotoxic stress and inducible chaperone networks in neurodegenerative disease and aging. Genes Dev. **22**, 1427–1438 (2008).
3. Marco, S., Carrascosa, J.L. & Valpuesta, J.M. Reversible interaction of beta-actin along the channel of the TCP-1 cytoplasmic chaperonin. Biophys J. **67**, 364–368 (1994).
4. Llorca, O., et al. Eukaryotic type II chaperonin CCT interacts with actin through specific subunits. Nature **402**, 693–696 (1999).
5. Zhu, Q.L., Wang, T.F., Cao, Q.F., Zheng, M.H.Lu, A.G. Inhibition of cytosolic chaperonin CCTζ-1 expression depletes proliferation & of colorectal carcinoma *in vitro*. J. Surg. Oncol. **102**, 419–423 (2010).
6. Cui, X., Hu, Z.P., Li, Z., Gao, P.J. & Zhu, J.Y. Overexpression of chaperonin containing TCP1, subunit 3 predicts poor prognosis in hepatocellular carcinoma. World J. Gastroenterol. **21**, 8588–8604 (2015).
7. Huang, X.D., et al. Chaperonin containing TCP1, subunit 8 (CCT8) is upregulated in hepatocellular carcinoma and promotes HCC proliferation. APMIS. **122**, 1070–1079 (2014).
8. Guest, S.T., Kratche, Z.R., Bollig-Fischer, A., Haddad, R. & Ethier, S.P. Two members of the TRiC chaperonin complex, CCT2 and TCP1 are essential for survival of breast cancer cells and are linked to driving oncogenes. Exp. Cell Res. **332**, 223–235 (2015).
9. Hallal, S., et al. Extracellular vesicles from neurosurgical aspirates identifies chaperonin containing TCP1 subunit 6A as a potential glioblastoma biomarker with prognostic significance. Proteomics **19**, e1800157 (2019).
10. Yang, J., et al. CCT α is a novel biomarker for diagnosis of laryngeal squamous cell cancer. Sci. Rep. **9**, 11823 (2019).

11. Liu, Y.J., Chang, Y.J., Kuo, Y.T. & Liang, P.H. Targeting β-tubulin/CCT-β complex induces apoptosis and suppresses migration and invasion of highly metastatic lung adenocarcinoma. Carcinogenesis **41**, 699–710 (2019).
12. Kasembeli, M., et al. Modulation of STAT3 folding and function by TRiC/CCT chaperonin. PLoS Biol. **12**, e1001844 (2014).
13. Bassiouni, R., et al. Chaperonin containing TCP-1 protein level in breast cancer cells predicts therapeutic application of a cytotoxic peptide. Clin. Cancer Res. **22**, 4366–4379 (2016).
14. Trinidad, A.G., et al. Interaction of p53 with the CCT complex promotes protein folding and wild-type p53 activity. Mol. Cell. **50**, 805–817 (2013).
15. Kim, A.R. & Choi, K.W. TRiC/CCT chaperonins are essential for organ growth by interacting with insulin/TOR signaling in Drosophila. Oncogene **38**, 4739–4754 (2019).
16. Roh, S.H., Kasembeli, M., Bakthavatsalam, D., Chiu, W. & Tweardy, D.J. Contribution of the type II chaperonin, TRiC/CCT, to oncogenesis. Int. J. Mol. Sci. **16**, 26706–26720 (2015).
17. Tang, N., Cai, X., Peng, L., Liu, H. & Chen, Y. TCP1 regulates Wnt7b/β-catenin pathway through P53 to influence the proliferation and migration of hepatocellular carcinoma cells. Signal Transduct Target Ther. **5**, 169 (2020).
18. Ray, D., Cuneo, K.C., Rehemtulla, A., Lawrence, T.S. & Nyati, M.K. Inducing Oncoprotein Degradation to Improve Targeted Cancer Therapy. Neoplasia **17**, 697–703(2015).
19. Gabay, M., Li, Y. & Felsher, D.W. MYC activation is a hallmark of cancer initiation and maintenance. Cold Spring Harb. Perspect. Med. **4**, a014241(2014).
20. Dang, C.V. MYC on the path to cancer. Cell **149**, 22–35 (2012).
21. Wirth, M., Mahboobi, S., Krämer, O.H. & Schneider, G. Concepts to Target MYC in Pancreatic Cancer. Mol. Cancer Ther. **15**, 1792–1798 (2016).
22. Wang, W., et al. SCP1 regulates c-Myc stability and functions through dephosphorylating c-Myc Ser62. 22. Oncogene **35**, 491–500 (2016).
23. Kandoth, C., et al. Mutational landscape and significance across 12 major cancer types. Nature **502**, 333–339 (2013).
24. Stokoe, D., et al. Dual role of phosphatidylinositol-3,4,5-trisphosphate in the activation of protein kinase B. Science **277**, 567–570 (1997).
25. Osaki, M., Oshimura, M. & Ito, H. PI3K-Akt pathway: its functions and alterations in human cancer. Apoptosis **9**, 667–676 (2004).
26. Cross, D.A., Alessi, D.R., Cohen, P., Andjelkovich, M. & Hemmings, B.A. Inhibition of glycogen synthase kinase-3 by insulin mediated by protein kinase B. Nature **378**, 785–789 (1995).
27. Sears, R., et al. Multiple RAS-dependent phosphorylation pathways regulate MYC protein stability. Genes Dev. **14**, 2501–2514 (2000).
28. Sears, R.C. The life cycle of C-myc: from synthesis to degradation. Cell Cycle **3**, 1133–1137 (2004).

29. Arnold, H.K., et al. The Axin1 scaffold protein promotes formation of a degradation complex for c-Myc. EMBO J. **28**, 500–512 (2009)..
30. Hydbring, P., et al. Phosphorylation by Cdk2 is required for Myc to repress Ras-induced senescence in cotransformation. *Proc. Natl. Acad. Sci. USA.* **107**, 58–63 (2010).
31. Bennett, J.M., et al. Proposed revised criteria for the classification of acute myeloid leukemia. A report of the French-American-British Cooperative Group. Ann. Intern. Med. **103**, 620–625 (1985).
32. Tan, F., et al. Identification of Isocitrate Dehydrogenase 1 as a Potential Diagnostic and Prognostic Biomarker for Non-small Cell Lung Cancer by Proteomic Analysis. Mol. Cell Proteomics.**11**, 111.008821 (2012).
33. Lian, X., et al. Pin1 inhibition exerts potent activity against acute myeloid leukemia through blocking multiple cancer-driving pathways. J. Hematol. Oncol. **11**, 73 (2018).
34. Yan, X., et al. MicroRNA-140-5p inhibits hepatocellular carcinoma by directly targeting the unique isomerase Pin1 to block multiple cancer-driving pathways. Sci. Rep. **7**, 45915 (2017).
35. Gallagher, R., et al. Characterization of the continuous, differentiating myeloid cell line (HL-60) from a patient with acute promyelocytic leukemia. Blood **54**, 713–733 (1979).
36. Liu, Y.J., Kumar, V., Lin, Y.F. & Liang, P.H. Disrupting CCT-β:β-tubulin selectively kills CCT-β overexpressed cancer cells through MAPKs activation. Cell Death Dis. **8**, e3052 (2017).
37. Showalter, A.E., et al. Investigating Chaperonin-Containing TCP-1 subunit 2 as an essential component of the chaperonin complex for tumorigenesis. Sci. Rep. **10**, 798(2020).
38. Yao, L., Zou, X. & Liu, L. The TCP1 ring complex is associated with malignancy and poor prognosis in hepatocellular carcinoma. Int. J. Clin. Exp. Pathol. **12**, 3329–3343 (2019).
39. Gao, H., et al. Chaperonin containing TCP1 subunit 5 is a tumor associated antigen of non-small cell lung cancer. Oncotarget **8**, 64170–64179 (2017).
40. Sternlicht, H., et al. The t-complex polypeptide 1 complex is a chaperonin for tubulin and actin *in vivo*. *Proc. Natl. Acad. Sci. USA.* **90**, 9422–9426 (1993)..
41. Vallin, J. & Grantham, J. The role of the molecular chaperone CCT in protein folding and mediation of cytoskeleton-associated processes: implications for cancer cell biology. Cell Stress Chaperones **24**, 17–27 (2019).
42. Feldman, D.E., Thulasiraman, V., Ferreyra, R.G. & Frydman, J. Formation of the VHL-elongin BC tumor suppressor complex is mediated by the chaperonin TRiC. Mol. Cell. **4**, 1051–1061 (1999).
43. Sherr, C.J. Cancer cell cycles. Science **274**, 1672–1677(1996).
44. Hanahan, D. & Weinberg, R.A. Hallmarks of cancer: the next generation. Cell **144**, 646–674 (2011).
45. Gurel, B., et al. Nuclear MYC protein overexpression is an early alteration in human prostate carcinogenesis. Mod. Pathol. **21**, 1156–1167 (2008).
46. Williams, K., et al. Unopposed c-MYC expression in benign prostatic epithelium causes a cancer phenotype. Prostate **63**, 369–384 (2005).

47. Wonsey, D.R., Zeller, K.I. & Dang, C.V. The c-Myc target gene PRDX3 is required for mitochondrial homeostasis and neoplastic transformation. *Proc. Natl. Acad. Sci. USA.* **99**, 6649–6654 (2002).
48. Koh, C.M., et al. MYC and Prostate Cancer. Genes Cancer **1**, 617–628 (2010).
49. Miller, D.M., Thomas, S.D., Islam, A., Muench, D. & Sedoris K. c-Myc and cancer metabolism. Clin. Cancer Res.**18**, 5546–5553 (2012).
50. Wang, Z., et al. lncRNA Epigenetic Landscape Analysis Identifies EPIC1 as an Oncogenic lncRNA that Interacts with MYC and Promotes Cell-Cycle Progression in Cancer. Cancer Cell **33**, 706–720.e9(2018).
51. Sviripa, V.M., et al. Halogenated diarylacetylenes repress c-myc expression in cancer cells. Bioorg. Med. Chem. Lett. **24**, 3638–40(2014).
52. Akinyeke, T., et al. Metformin targets c-MYC oncogene to prevent prostate cancer. Carcinogenesis **34**, 2823–2832 (2013).
53. Janghorban, M., et al. Targeting c-MYC by antagonizing PP2A inhibitors in breast cancer. *Proc. Natl. Acad. Sci. USA.* **111**, 9157–9162 (2014).
54. Ramsay, G., Evan, G.I. & Bishop, J.M. The protein encoded by the human proto-oncogene c-myc. Proc Natl Acad Sci USA. **81**, 7742–7746 (1984).
55. Tsai, W.B., et al. Activation of Ras/PI3K/ERK Pathway Induces c-Myc Stabilization to Upregulate Argininosuccinate Synthetase, Leading to Arginine Deiminase Resistance in Melanoma Cells. Cancer Res. **72**, 2622–2633 (2012).
56. Welcker, M., et al. The Fbw7 tumor suppressor regulates glycogen synthase kinase 3 phosphorylation-dependent c-Myc protein degradation. Proc Natl Acad Sci USA. **101**, 9085–9090 (2004).
57. Bowles, D.W. & Jimeno, A. New phosphatidylinositol 3-kinase inhibitors for cancer. Expert Opin. Investig. Drugs **20**, 507–518 (2011).
58. Pal, S.K., Reckamp, K., Yu, H. & Figlin, R.A. Akt inhibitors in clinical development for the treatment of cancer. Expert Opin. Investig. Drugs **19**, 1355–1366 (2010).
59. Chin, L., Andersen, J.N. & Futreal, P.A. Cancer genomics: from discovery science to personalized medicine. Nat. Med. **17**, 297–303 (2011).

Figures

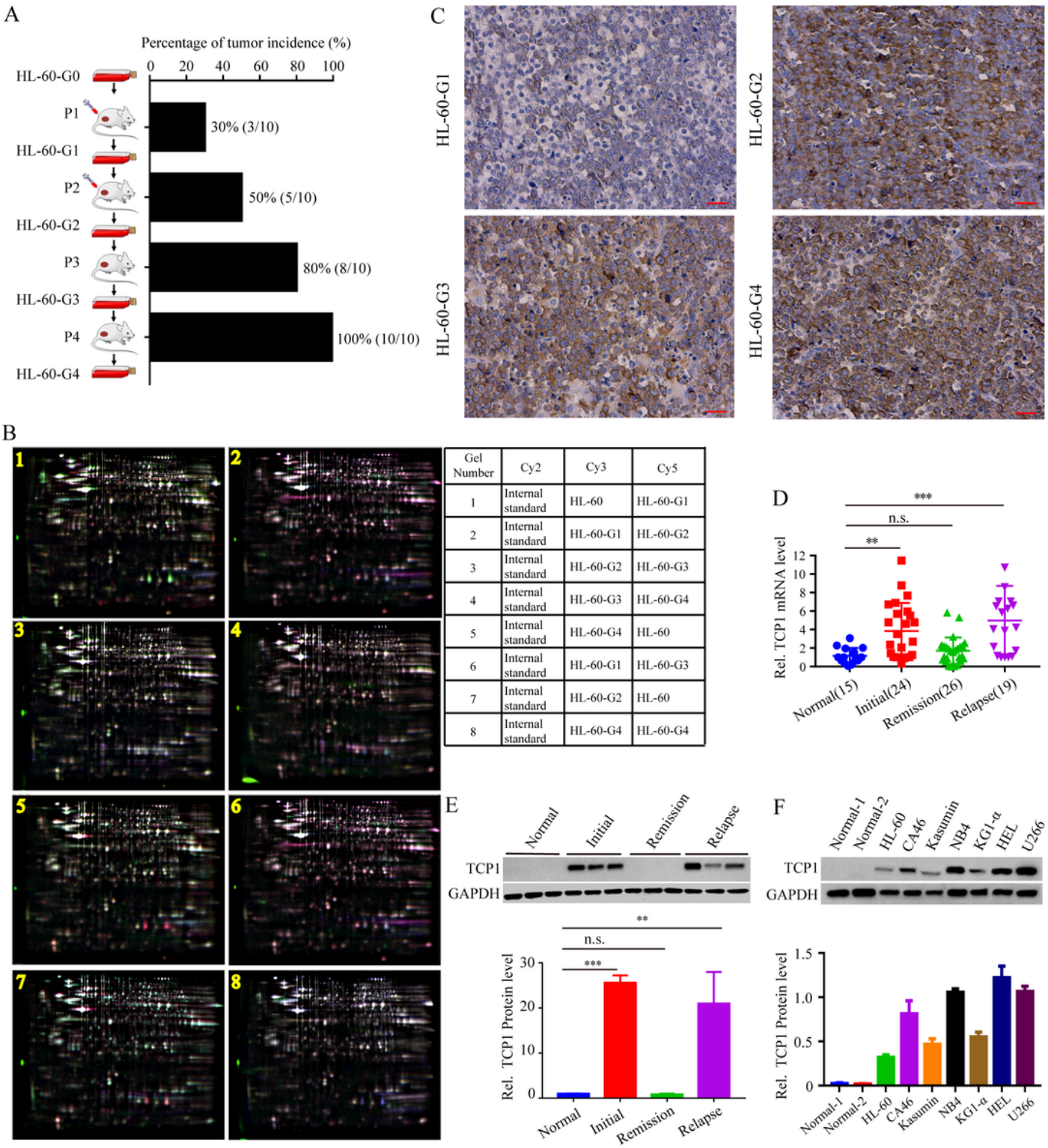

Figure 1

TCP1 is upregulated and positively correlated with the occurrence of AML. **a.** The percentage of tumor incidence in the HL-60 cell line increased with generation. The rates of tumorigenesis were 3/10, 5/10, 8/10, and 10/10. **b.** Two-dimensional in-gel electrophoresis combined with mass spectrometry targeted TCP1 as a highly oncogenic gene. **c.** The expression of TCP1 in HL-60 cells was increased by generation, and the results are shown by representative IHC images. Scale bar, 200 μm. **d, e.** The expression of TCP1

in the primary AML, remission, relapse, and control groups was detected by RT-PCR (d) and WB (e). **f.** The expression of TCP1 in various leukemia cell lines. Data are shown as the mean ± SD from three independent experiments. *$P < 0.05$, **$P < 0.01$, ***$P < 0.001$, between the indicated groups.

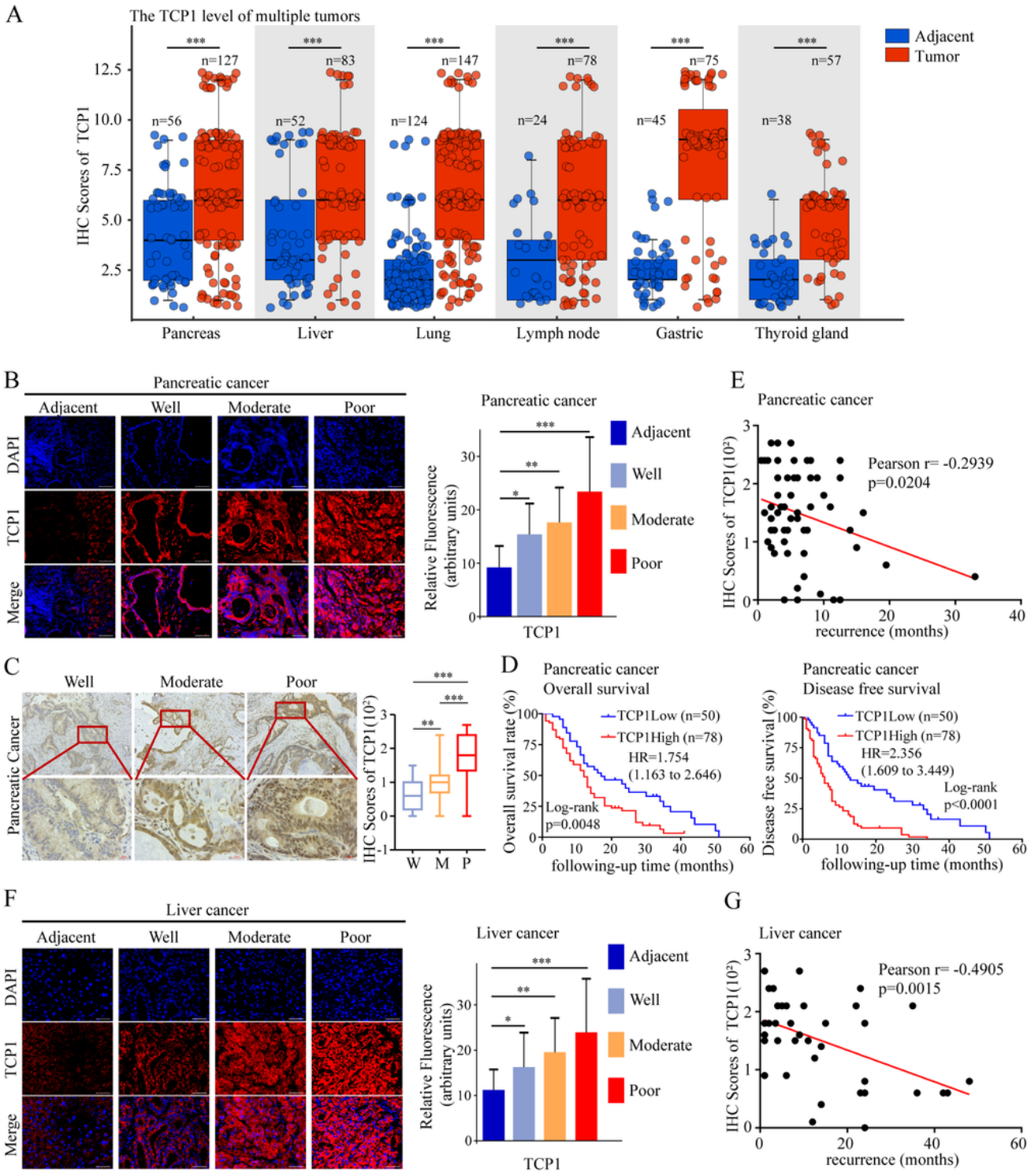

Figure 2

TCP1 is highly expressed in malignant tumors and predicts a poor prognosis. **a.** IHC was carried out, and the relative TCP1 staining intensity was scored to analyze the expression of TCP1 in adjacent and malignant tumors. **b, c, f.** Fluorescence imaging and IHC were used to assay the relationship between the expression of TCP1 and the degrees of differentiation in pancreatic and liver cancers. Representative images and the relative scores of TCP1 are shown in pancreatic cancer (b,c) and liver cancer (f). Scale bar, 200 μm. **d.** The relationship between the expression of TCP1 and pancreatic cancer patients' overall and disease-free survival rates. **e, g.** The relationship between TCP1 levels and the recurrence time of pancreatic cancer (e) and liver cancer (g). Data are shown as the mean ± SD from three independent experiments. $*P < 0.05$, $**P < 0.01$, $***P < 0.001$, between the indicated groups.

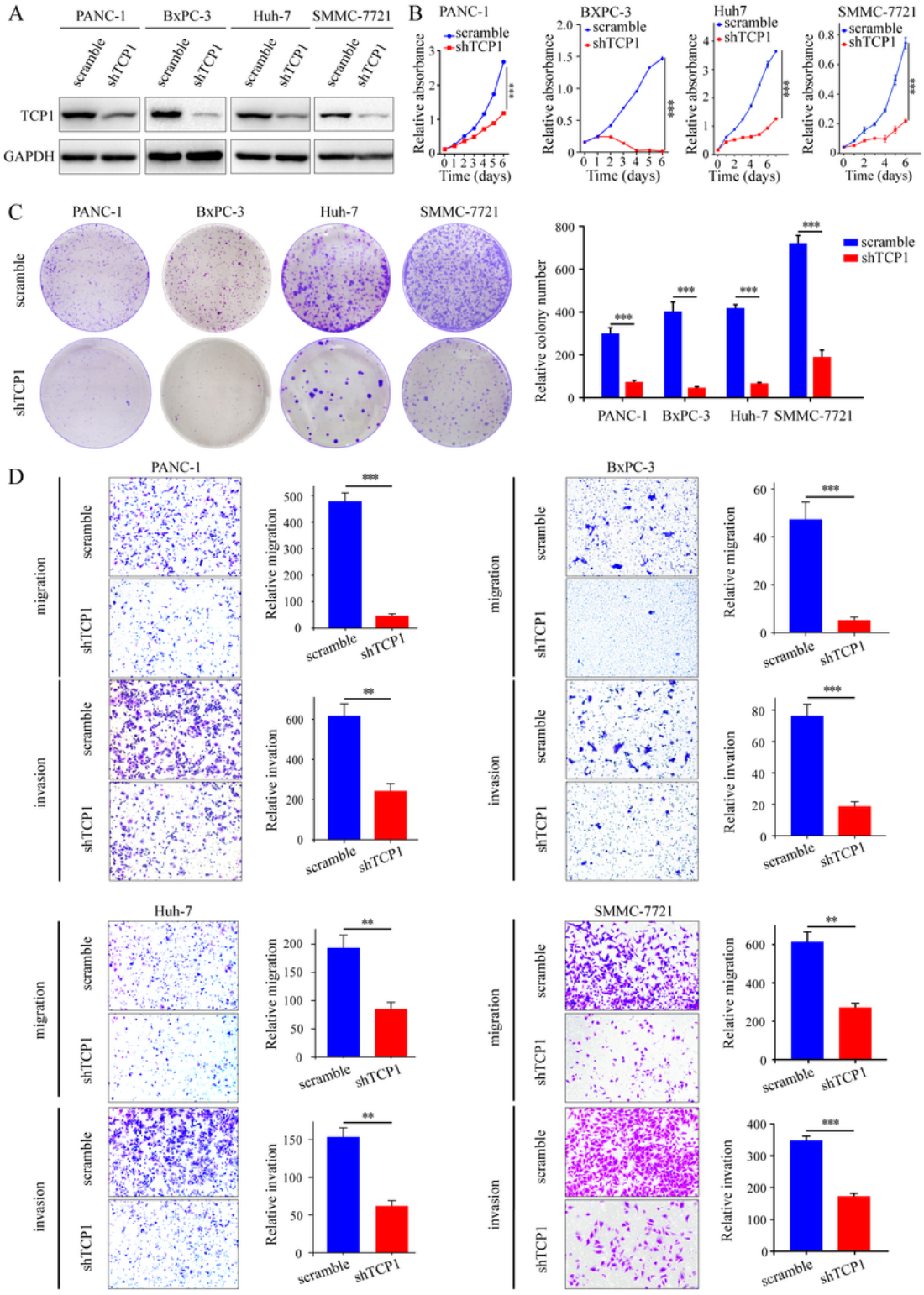

Figure 3

TCP1 promotes the proliferation and metastasis of PDAC and HCC cells *in vitro*. **a.** A lentiviral system was applied to induce the stable expression of shRNA targeting TCP1, and TCP1 expression was detected by WB. **b,c.** MTT (b) and colony formation (c) assays were used to assay the cell growth ability of PANC-1, BxPC-3, Huh-7, and SMMC-7721 cells. **d.** Transwell assays were carried out to analyze the migration

and invasion ability of cells. Data are shown as the mean ± SD from three independent experiments. *P < 0.05, **P < 0.01, ***P < 0.001, between the indicated groups.

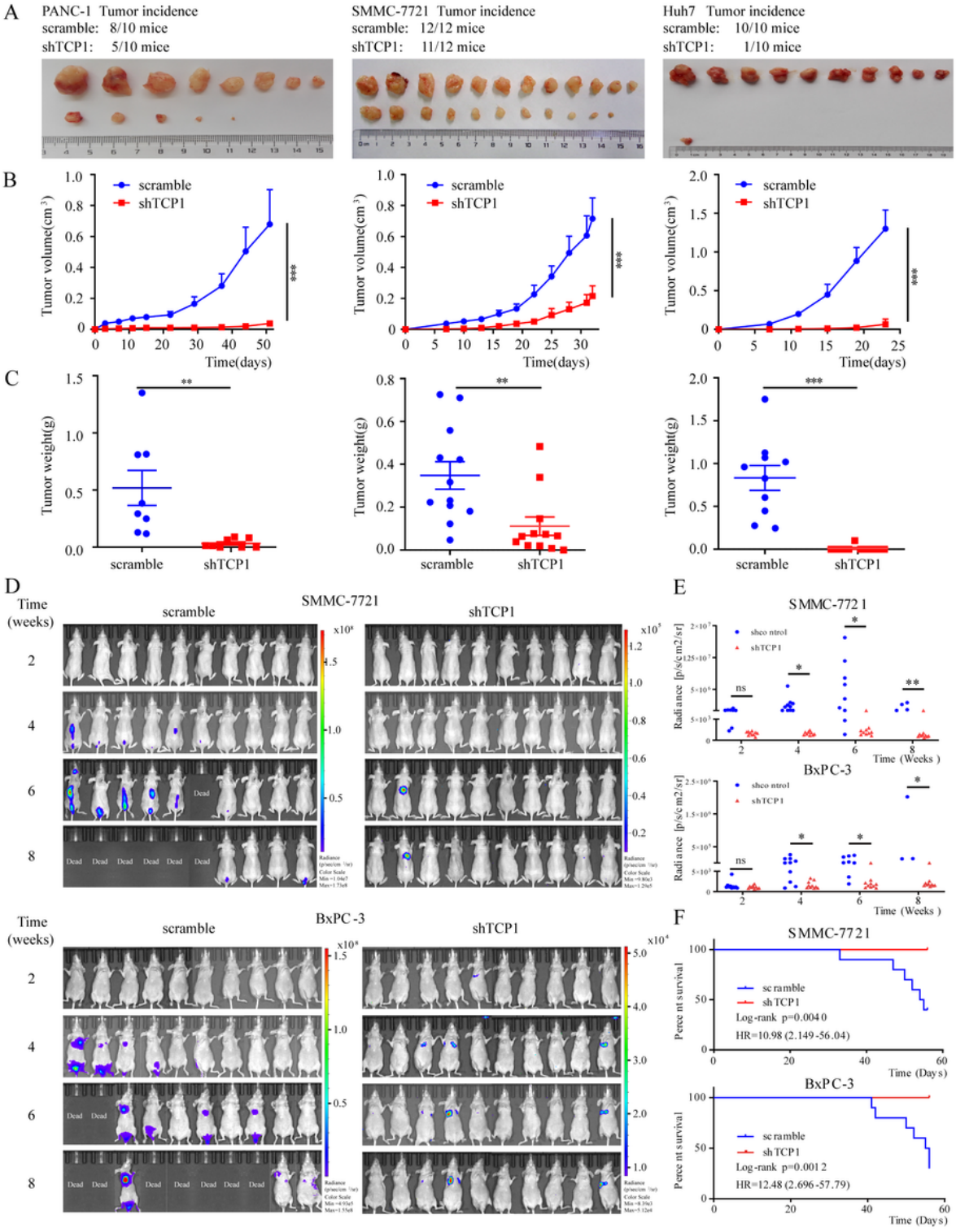

Figure 4

Repression of TCP1 inhibits the proliferation and metastasis of pancreatic and hepatoma cells *in vivo*. **a, b, c.** The tumor volume and tumor weight of the xenograft mouse model were measured and analyzed.

Images of tumors (a) and the tumor volume (b) and tumor weight (c) are shown. **d, e, f.** A living imaging system for small animals was used to assay the metastatic ability of pancreatic cancer and liver cancer cells *in vivo* (d). The intensity of radiance was summarized (e). Mice survival was further analyzed (f). Data are shown as the mean ± SD from three independent experiments. **P* < 0.05, ***P* < 0.01, ****P* < 0.001, between the indicated groups.

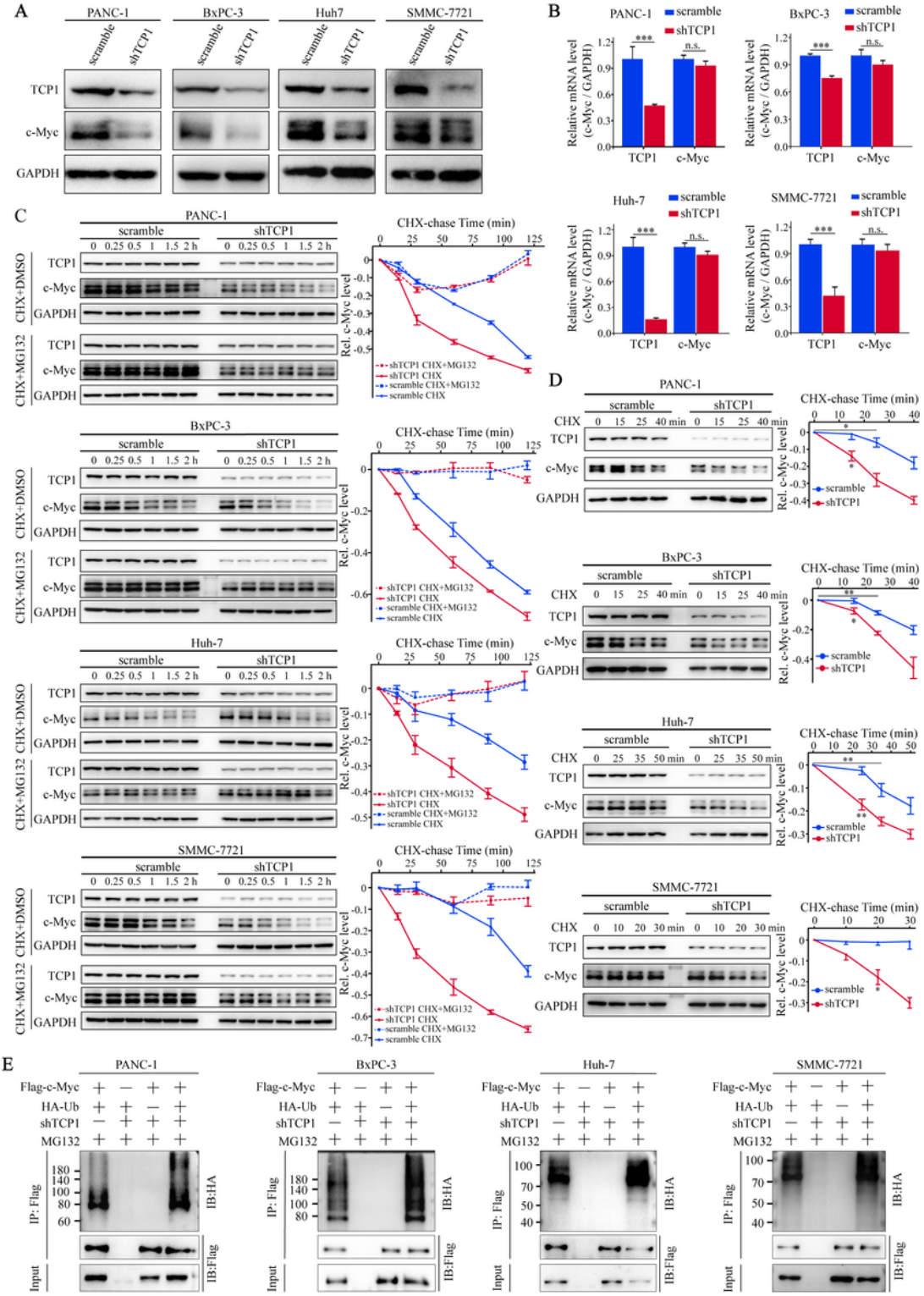

Figure 5

TCP1 regulates the stability of c-Myc through the ubiquitin-proteasome pathway. **a, b.** TCP1 was knocked down, and the expression of c-Myc and TCP1 in PANC-1, BxPC-3, Huh-7, and SMMC-7721 cells was detected by WB (a) and RT-qPCR (b). **c, d.** Cells were treated with 50 μM CHX and 10 μM MG132 or DMSO. The protein levels of TCP1 and c-Myc were determined by WB assays (c). PANC-1 cells and BxPC-3 cells were treated with CHX for 0, 15, 25, and 40 min. Huh-7 cells were treated with CHX for 0, 30, 40, and 50 min. SMMC-7721 cells were treated with CHX for 0, 10, 20, and 30 min. Then, the protein levels of TCP1 and c-Myc were determined by WB assays, and the relationship between CHX chase time and relative c-Myc level was analyzed (d). **e.** Ubiquitination assays were carried out to observe the ubiquitination level of c-Myc in the shTCP1+Flag-c-Myc+HA-ubiquitin+MG132 group and scramble+Flag-c-Myc+HA-ubiquitin+MG132 group. Data are shown as the mean ± SD from three independent experiments. *$P < 0.05$, **$P < 0.01$, ***$P < 0.001$, between the indicated groups.

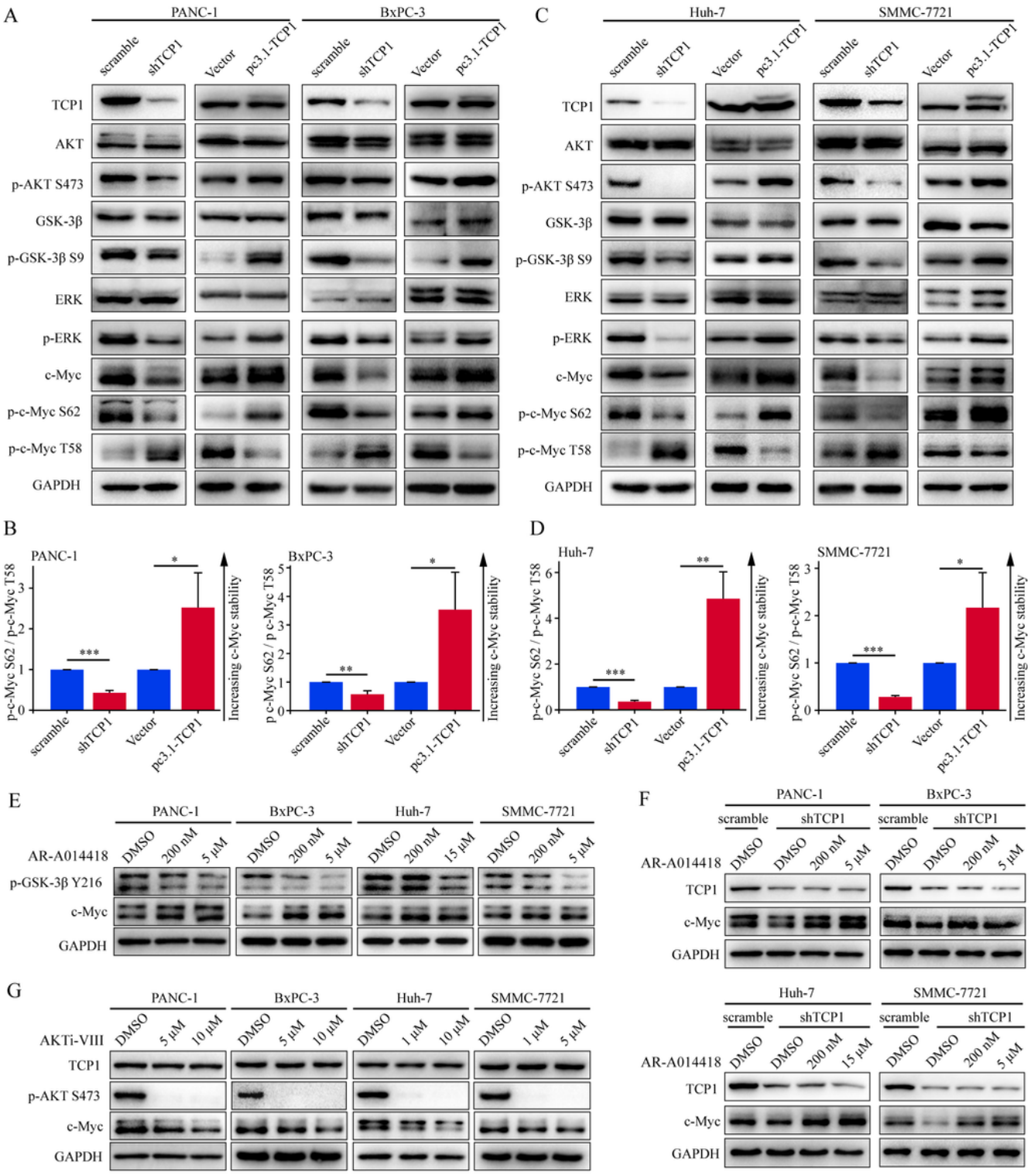

Figure 6

The influence of TCP1 knock-down on the stability of c-Myc and AKT/GSK-3β and ERK signaling pathway components. **a-d.** TCP1 was knocked down, and then the levels of c-Myc, p-c-Myc Thr58, p-c-Myc Ser62, TCP1, AKT, p-AKT Ser473, GSK-3β, and p-GSK-3β Ser9 in PANC-1 and BxPC-3 cells were detected by WB (a, b). The same detection markers were assessed in Huh-7 and SMMC-7721 cells (c, d). **e.** The GSK-3β inhibitor AR-A014418 was used to confirm the effect of TCP1 on the AKT/GSK-3β axis. PANC-1, BxPC-3,

and SMMC-7721 cells were treated with 200 nM and 5 μM AR-A014418, and Huh-7 cells were treated with 200 nM and 15 μM AR-A014418; then, the levels of p-GSK-3β Y216 and c-Myc were detected. **f.** AR-A014418 was used in scramble and shTCP1 cells to measure the level of c-Myc protein. **g.** AKT inhibitor VIII (AKT iVIII) was used to determine the relationship between TCP1 and the AKT/GSK-3β pathway. PANC-1 and BxPC-3 cells were treated with 5 μM and 10 μM AKT iVIII, Huh-7, and SMMC-7721 cells were treated with 1 μM and 10 μM AKT iVIII, and the expression of TCP1, p-AKT Ser473 and c-Myc was detected. Data are shown as the mean ± SD from three independent experiments. *$P < 0.05$, **$P < 0.01$, ***$P < 0.001$, between the indicated groups.

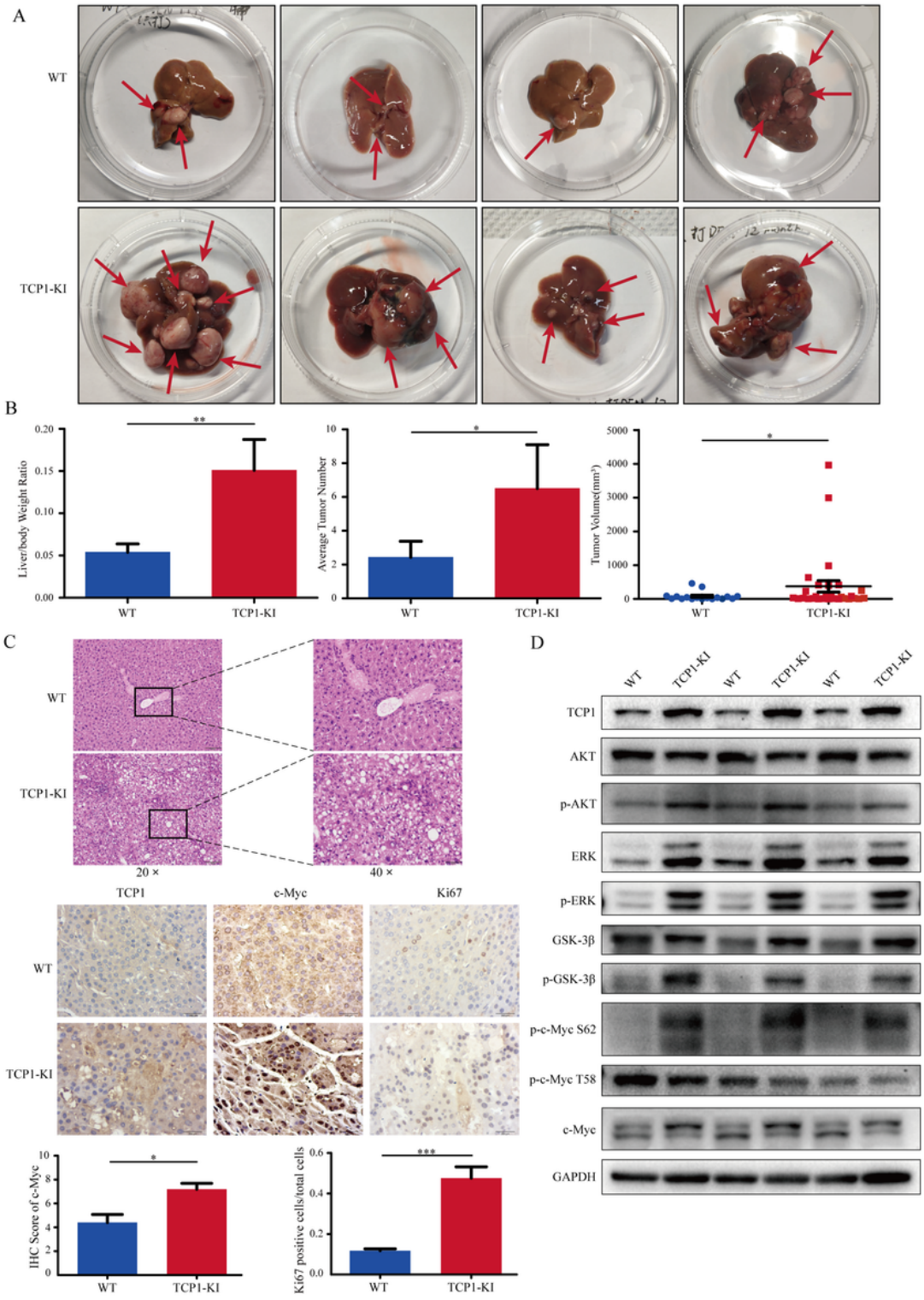

Figure 7

TCP1 promotes the development of HCC and regulates AKT/GSK-3β and ERK signaling pathways. **a, b.** The number of tumor nodules (the red arrows), liver weight ratio, and tumor volume of WT and TCP1-KI mice were calculated and analyzed. Images of hepatomas (a), the liver/body weight ratio, the tumor number, and the tumor volume are shown (b). **c.** HE staining and IHC were carried out to observe the structure of liver tissues and assay the levels of TCP1, c-Myc, and Ki67. Scale bar, 200 μm. **d.** c-Myc, p-c-

Myc Thr58, and p-c-Myc Ser62 and AKT, p-AKT Ser473, GSK-3β, p-GSK-3β Ser9, p-ERK, and ERK in mouse tissues were detected to determine the effect of overexpressing TCP1 *in vivo*. Data are shown as the mean ± SD from three independent experiments. **P* < 0.05, ***P* < 0.01, ****P* < 0.001, between the indicated groups.

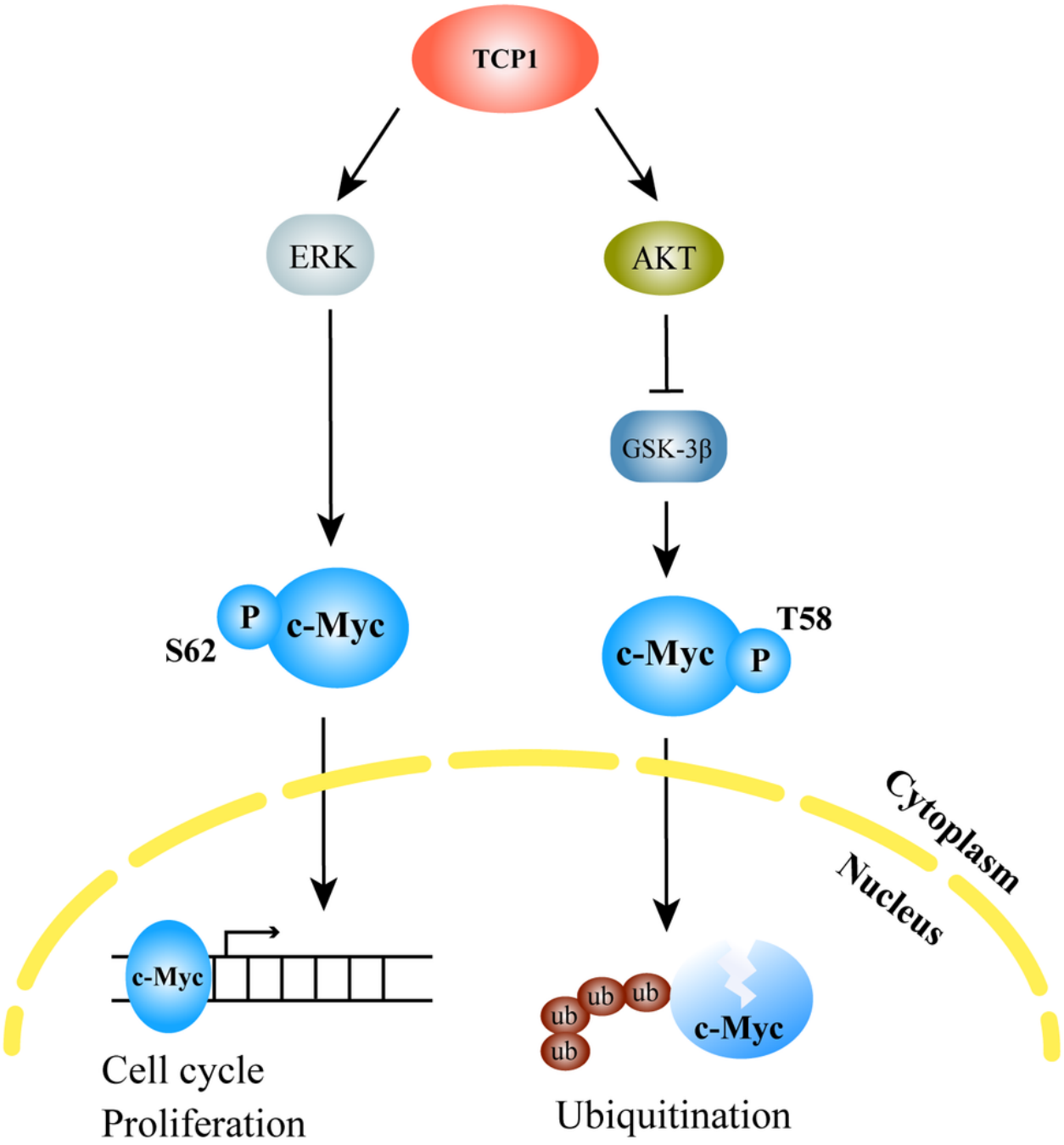

Figure 8

A proposed model of the mechanism of TCP1. TCP1 activates the ERK axis and then affects the phosphorylation of c-Myc Ser62, which increases the stability of c-Myc and enhances cell proliferation and metastasis. In addition, TCP1 knock-down inhibits the function of the AKT/GSK-3β pathway, which can phosphorylate c-Myc Thr58 and accelerate degradation via the ubiquitin-proteasome pathway.

Supplementary Files

This is a list of supplementary files associated with this preprint. Click to download.

- Supplementaryinformationfile.pdf
- SupplementaryFigure2.tif
- supplementaryFigure1.tif
- SupplementalTableS1.docx
- SupplementalTableS2.docx